Effects of Swirl and High Turbulence on a Jet in a Crossflow

M. S. Kavsaoglu* and J. A. Schetz†
Virginia Polytechnic Institute and State University, Blacksburg, Virginia

An experimental study has been conducted on the effects of initial swirl and high turbulence in the exhaust of a circular jet injected from a flat plate at a 90-deg angle into a crossflow. The different jet types studied were low-exit turbulence (3%), high-exit turbulence (>10%), and 40 and 58% swirl. Surface pressure distributions and mean velocity vector plots were obtained for all of these cases. For the surface pressure distribution tests, the jet to crossflow velocity ratios R were 2.2, 4, and 8 for most of the jet types. For the mean velocity vector plots, $R=4$ was chosen. Turbulence information in the jet plume was also obtained for the low-exit turbulence case at $R=4$. The results showed that the higher-exit turbulence reduced the penetration height, and it also reduced the surface area influenced by negative pressures. The swirl-caused asymmetric pressure distributions and the swirl effects were more pronounced for lower-velocity ratios.

Nomenclature

A	= area
C_p	= pressure coefficient
ΔC_p	$= C_{p_{\text{jet on}}} - C_{p_{\text{jet off}}}$
D	= jet exit diameter
p	= static presssure, pressure
q	= dynamic pressure
R	= jet-to-crossflow velocity ratio
X,Y,Z	= Cartesian coordinates
U,V,W	= velocity components
u',v',w'	= fluctauting velocity components
U_{TOT}	= total velocity
Subscripts	
j	= jet
∞	= freestream

Introduction

CROSSFLOW jet injection has numerous applications—fuel injection into combustion chambers, film cooling, and the transition flight of VTOL aircraft, among others. There is a large number of parameters involved in this general problem: jet-to-crossflow velocity ratio, jet injection angle, jet shape, side-by-side or tandem multiple jets, temperature differences between the jet and crossflow, Reynolds and Mach numbers, multiphase flows, jet exit velocity and turbulence profiles, swirl, etc. Much research has been done in this area, and reviews[1-7] show that majority were experimental. In addition to the widely studied case of single circular jet normal to a crossflow,[6,7,12-19] dual jets,[7,11,24] injection from a body of revolution,[8] nonuniform velocity profiles,[10,14,19] rectangular jets,[7,11,23] and jet injection angle,[7-9,11,24] have also been studied. Throughout the years, prediction methods have also been improved.[20-22] In spite of all this prior work, jet exit turbulence level and swirl have received little or no previous attention.[5] These effects are significant for the VTOL aircraft application and others. Furthermore, a study on the effects of jet exit turbulence level can also be useful to explain some of the apparent scatter in the results of previous experimental studies.

The general features of these flowfields are known.[1-5] A jet injected at a right angle into a crossflow bends toward the downstream under the effect of crossflow. The core of the jet takes a kidney-like shape. Two contrarotating bound vortices form at the rear side of the jet. The crossflow passing the jet separates forming a wake region. A small positive pressure region forms in front of the jet due to blockage, and a large negative pressure region forms at the sides and to the rear. Also, air from the crossflow is accelerated by the jet through viscous entrainment, and this also causes negative pressures around the jet. This effect is more pronounced for higher-velocity ratios.

The test matrix for the present research can be seen in Table 1. In this work for a 90-deg circular jet, the effects of different jet exit velocity profiles and jet exit turbulence levels were studied. Jet types were 1) low-turbulence (3%), uniform profile, 2) high-turbulence (>10%), uniform profile, and 3) swirling. Swirl ratios of 40 and 58% were studied. Here we have defined "swirl ratio" as the maximum peripheral velocity near the nozzle wall divided by the average axial velocity. Results were obtained as surface pressure distributions, mean velocity vector plots, and turbulence intensities and Reynolds stresses. Surface pressure distribution tests were done for jet-to-crossflow velocity ratios R of 2.2, 4, and 8. The ratio $R=8$ was omitted for the high-turbulence case due to the very low crossflow velocity needed. Mean velocity vector plots were obtained for $R=4$. Turbulence intensities and Reynolds stresses in the jet plume were obtained for $R=4$ on the centerplane of the low-exit turbulence case.

Apparatus

The experiments were carried out in the 6 ft × 6 ft (1.83 m × 1.83 m) Stability Tunnel at Virginia Polytechnic Institute.[7] This is a closed-circuit tunnel with a 24 ft (7.32 m) long test section and a very low-turbulence flow.

The jet was injected from a 1.78 m × 2.13 m flat plate model that was large compared to the jet diameter (49.2 mm). The plate had a rounded leading edge and a tapered trailing edge. The jet was exhausted downward at 19 in. (48.3 cm) behind the leading edge. There was a sandpaper strip glued at 4.5 in. (11.4 cm) back from the leading edge to keep the boundary layer turbulent at low tunnel velocities. This was confirmed by boundary layer profile measurements. An area of 12 in. × 16 in. (30.48 cm × 40.64 cm) was covered with more than 450 pressure taps. These taps were located at the intersections of the parallel lines in X and Y directions (see Fig. 3

Received March 3, 1988; revision received Nov. 11, 1988.

*Graduate Research Assistant, Aerospace and Ocean Engineering Department; currently at Department of Aeronautical Engineering, Middle East Technical University, Ankara, Turkey. Member AIAA.

†W. Martin Johnson Professor and Department Head, Aerospace and Ocean Engineering Department. Fellow AIAA.

Table 1 Scope of the present research

Jet type	Jet velocity profile	Jet velocity m/s	U_j/U_∞ Pressure data	U_j/U_∞ Mean flow data	U_j/U_∞ Turbulence data
90-deg single circular	Uniform	62	2.2, 4, 8	4	4
90-deg single circular, high turbulence	Uniform	35	2.2, 4	4	—
90-deg single circular, 40% swirl	Swirling nozzle	62	2.2, 4, 8	4	—
90-deg single circular, 58% swirl	Swirling nozzle	62	2.2, 4, 8	4	—

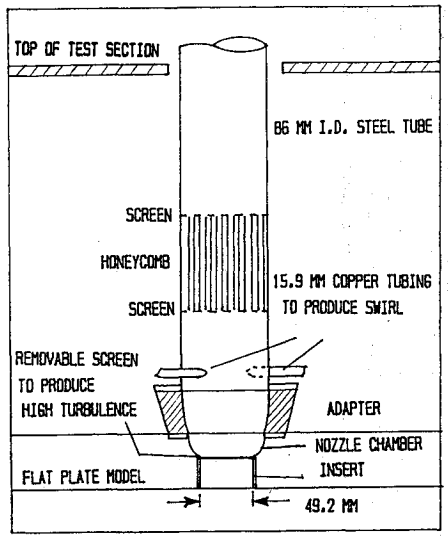

Fig. 1 Jet nozzle assembly

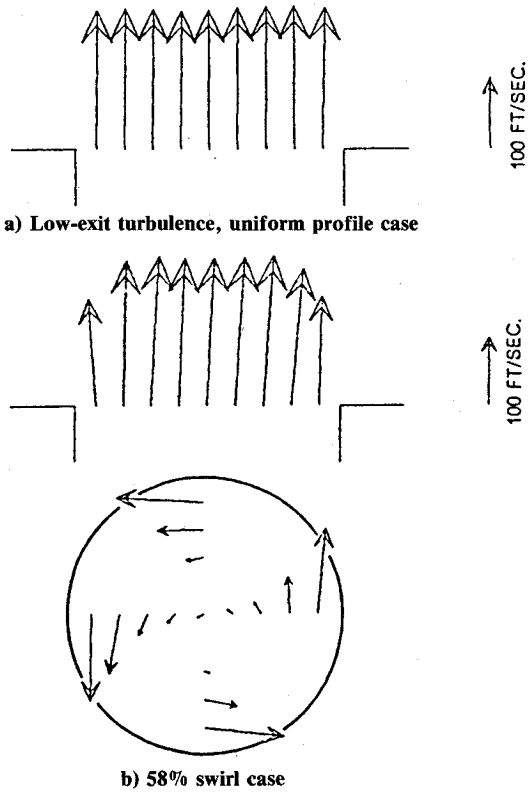

Fig. 2 Jet exit velocity profiles

for X and Y). Spacing between the taps was 0.85 cm in a 4 in. $\times$ 4 in. (10.16 cm $\times$ 10.16 cm) area just around the jet exit. For the rest of the area, spacing was 1.69 cm in both directions (see Refs. 7 and 22 for a figure example).

The jet nozzle assembly can be seen in Fig. 1. The jet exit diameter was 49.2 mm, and the flow was produced by an electric blower. Before injection, air passed through a 8.6-cm-diam steel tube 50 cm long, inside which there was a 5-cm-long honeycomb. At the end of this tube, a pair of 1.59-cm copper tubes were connected for tangential air injection to produce swirl. For nonswirling jet experiments the exits of these tubings were closed. Tangential air was supplied from 8.0-atm tanks and regulated through valves. The steel tube was followed by a 2.38-cm-long contraction and a 3-cm-long, 49.2-mm-diam constant area section before the jet exit. For the high-turbulence jet experiments, a turbulence-generating screen was placed right after the contraction and before the final constant area section.

Twelve transducers each connected to a 48-port Scanivalve were used for the pressure distribution experiments. A three-dimensional, yawhead probe was used to obtain mean flowfield measurements in the plumes of the jets. This probe was 61 cm long and had a 3.2-mm-diam for the first 5 cm from the tip. For the rest of the probe, the diameter was 6.4 mm. A normal, single, hot-wire probe was used for measuring the jet exit turbulence levels when there was no crossflow. Turbulence intensities and Reynolds stresses in the plume of the low-exit turbulence jet were measured with an X-wire probe. Two constant temperature anemometers, two linearizers, and a turbulence correlator were used. A probe rotator mechanism was utilized to align the hot wire with the mean flow direction and also to change roll angle in order to obtain all six of the turbulence quantities. The computerized data acquisition system of the wind tunnel was used to gather the various experimental data and store them on magnetic disks.

Test Conditions

During the experiments, the jet exit velocity was kept constant at about 220 ft/s (67 m/s) for the low-turbulence and swirling jets, and the crossflow velocity was adjusted according to jet-to-crossflow velocity ratio. The jet exit velocity was 115 ft/s (35 m/s) for the high-exit turbulence case due to the additional drag caused by the turbulence generating screen. The freestream velocity was changed from 28 ft/s (8.52 m/s) to 102 ft/s (31.04 m/s) depending on the velocity ratio. The freestream turbulence intensity was around 0.04%. The Reynolds number based on the jet diameter and the freestream velocity was 2.56×10^4 for the 28 ft/s freestream velocity, and 9.36×10^4 for the 102 ft/s freestream velocity. The Reynolds number at the nozzle, based on flat plate length up to this point, was 2.5×10^5 for the 28 ft/s freestream velocity and 9.1×10^5 for the 102 ft/s freestream velocity. The boundary-

layer profile at the nozzle location was always turbulent due to the sandpaper strip glued in front of the model. This boundary-layer profile at 28 ft/s freestream velocity was previously published[24] for the same model, showing the turbulent nature.

Jet exit mean velocity profiles were uniform for the low-exit turbulence and high-exit turbulence jets. The exit turbulence level for the low-turbulence case was 3% and uniformly distributed. For the high-turbulence case, the intensity was about 10% in the center and somewhat higher at the periphery (>16%). For swirling jets, the swirl ratio was defined as the ratio of the swirl component of the velocity at the periphery ($X/D=0.4$) to average total velocity. The exit velocity profiles for the low-exit turbulence case and the 58% swirl case are given in Fig. 2.

Experimental Techniques

A coordinate system was chosen for data presentation with the X axis aligned with the crossflow direction and the Z axis with the jet direction. A Y axis completed the right-hand system (see Fig. 3).

For the surface pressure distribution tests, tare readings were first obtained by running the tunnel with the jet off and the jet exit area covered flush with the model surface. Then, pressure readings were obtained again by running the tunnel with the jet on. The tare readings served to zero-out any flow disturbances caused by any small irregularities on the surface of the model. Nondimensional pressure coefficients

$$C_p = (p - p_\infty)/q_\infty$$

were obtained for jet-on and jet-off cases, and the data are presented as

$$\Delta C_p = (C_{p_{\text{jet on}}} - C_{p_{\text{jet off}}})$$

For the mean velocity vector plots, the yawhead probe was kept at a 45-deg angle with respect to the model surface. Probe calibration up to 60-deg angularities was available, and maximum flow angularities with respect to the probe were about 50 deg.

For the turbulence measurements, the local mean flow directions were known from the previously made yawhead measurements. At each measurement location, the X-wire probe was first aligned with the mean flow direction by changing the pitch angle of the probe. Then, data was read at 0, 90 and 45-deg roll angles of the probe. The normalization was made with the local total mean velocity.

Results

In this section, results of the surface pressure distribution, mean flowfield, and turbulence in the jet plume experiments will be presented. Pressure distribution measurements were made for low turbulence, high turbulence, and swirling jets with two swirl ratios at three different velocity ratios ($R=2.2$, 4, and 8). Mean flowfield measurements were also made for these jet types at $R=4$. Turbulence measurements were made only for the low-turbulence jet at $R=4$.

Pressure Distribution Measurements

The pressure distribution results are presented here as ΔC_p isobars. Thin isobar lines are drawn with $\Delta C_p=0.2$ intervals, and thick isobars lines are drawn with $\Delta C_p=1.0$ intervals.

Low-Exit Turbulence Jet

Pressure distribution results for this baseline configuration are presented in Figs. 3–5 for $R=2.2$, 4, and 8, respectively. Jet exit turbulence level for this jet was about 3% and distributed uniformly. The general features of the jet in a crossflow problem can be observed easily. Blockage of the crossflow by the jet induces a positive pressure region in front of the jet. Flow separation and formation of a pair of bound vortices induce a negative pressure region that extends toward the lateral and downstream directions. Viscous entrainment of the crossflow by the jet accelerates the crossflow toward the jet, and this also induces negative pressures around the jet. By increasing the velocity ratio, the negative pressure areas enlarge and move upstream. The maximum magnitudes of the negative pressures at the left and right sides of the jet were about −3, −5, and −4 for $R=2.2$, 4, and 8, respectively.

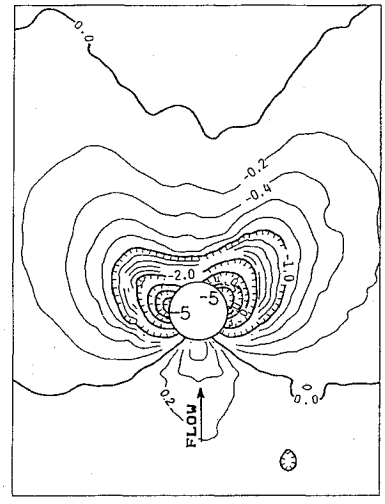

Fig. 4 Surface pressures, low-turbulence jet, $R=4.0$

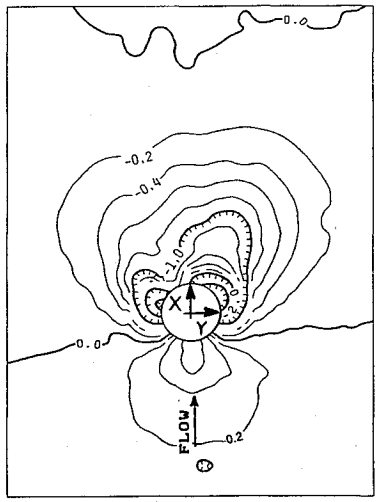

Fig. 3 Surface pressures, low-turbulence jet, $R=2.2$

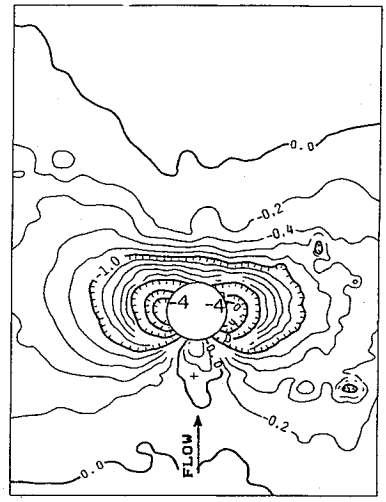

Fig. 5 Surface pressures, low-turbulence jet, $R=8.0$

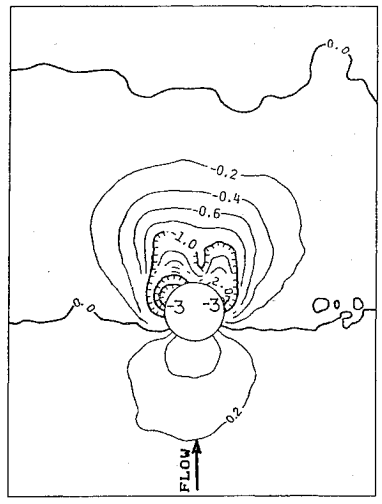

Fig. 6 Surface pressures, high-turbulence jet, $R=2.2$

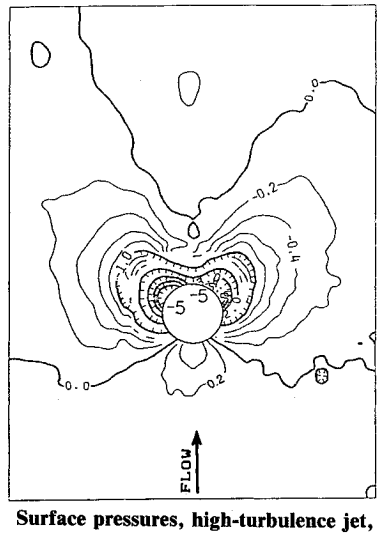

Fig. 7 Surface pressures, high-turbulence jet, $R=4.0$

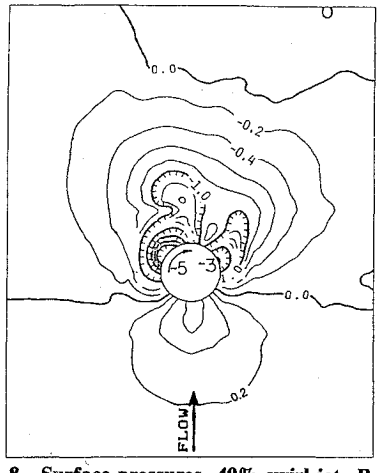

Fig. 8 Surface pressures, 40% swirl jet, $R=2.2$

Some asymmetry can be observed for the low-velocity ratios, particularly for $R=2.2$ (Fig. 3). This might be due to some weak vortex formation from the blower and the increased sensitivity of the flowfield to small imperfections at low-velocity ratios.

High-Exit Turbulence Jet

Pressure distribution results for the high-turbulence jet are presented in Figs. 6 and 7 for $R=2.2$ and 4, respectively. For this jet, exit turbulence intensity was about 10% in the center

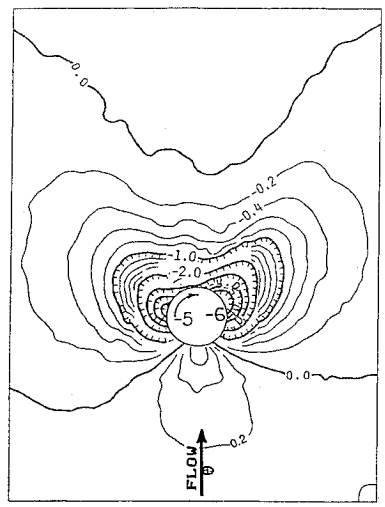

Fig. 9 Surface pressures, 40% swirl jet, $R=4.0$

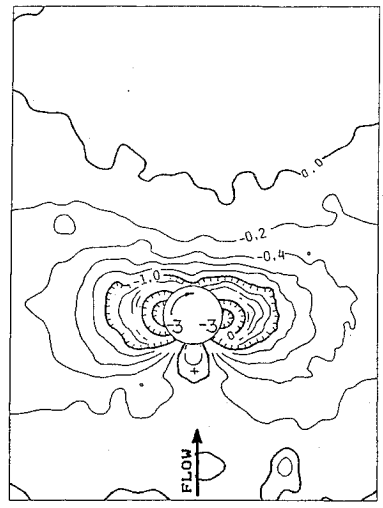

Fig. 10 Surface pressures, 40% swirl jet, $R=8.0$

and higher (>16%) at the periphery. By increasing the jet exit turbulence, the size of the negative pressure area was reduced (compare the $\Delta C_p=0.0$, -0.2, and -1.0 lines for the same velocity ratios from Figs. 3 and 4 vs Figs. 6 and 7). The maximum magnitudes of negative pressures did not seem to change for $R=2.2$, which are between -3.0 and -4.0 for both the low- and high-exit turbulence cases. The same is true for $R=4$. For this velocity ratio, the maximum magnitudes are between -5.0 and -6.0 for both cases. Since the maximum magnitudes did not change, but the area around them reduced, the decay of negative pressures is, obviously, faster for the high-turbulence case. It seems that increasing exit turbulence also helped to produce more symmetric pressure distributions (compare the -1.0 lines for $R=2.2$ from Figs. 3 and 6). This can be attributed to "mixing out" of any small nonuniformities in the jet exit flow.

Jet with Swirl

Pressure distribution results for the jet with swirl are presented in Figs. 8–13. These tests were carried out for two different swirl ratios (40 and 58%) and three different velocity ratios ($R=2.2$, 4, and 8) for each swirl ratio. In Fig. 8, for 40% swirl and $R=2.2$, a strongly asymmetric pressure distribution because of the swirl can be observed. Around the left rear side of the jet, the maximum negative pressures are between -5 and -6. However, the maximum negative pressure is about -3 around the right rear side. By increasing the velocity ratio to 4 and 8, the asymmetric pressure distributions due to swirl cannot be observed any more for the 40% swirl case (Figs. 9 and 10).

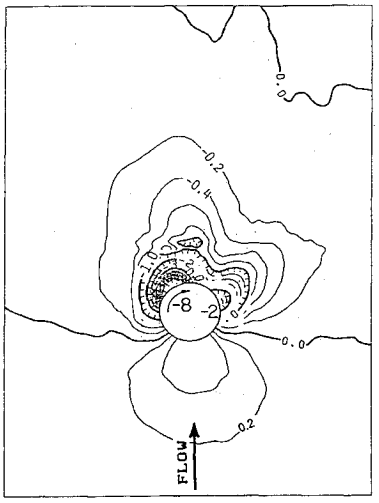

Fig. 11 Surface pressures, 58% swirl jet, $R=2.2$

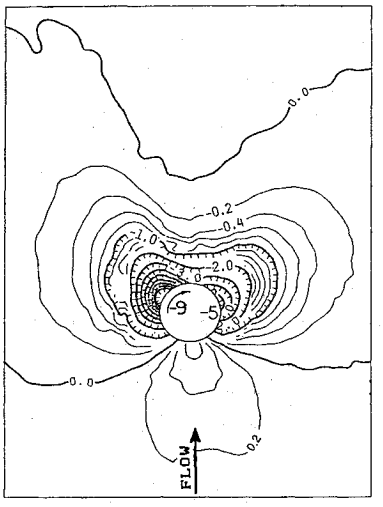

Fig. 12 Surface pressures, 58% swirl jet, $R=4.0$

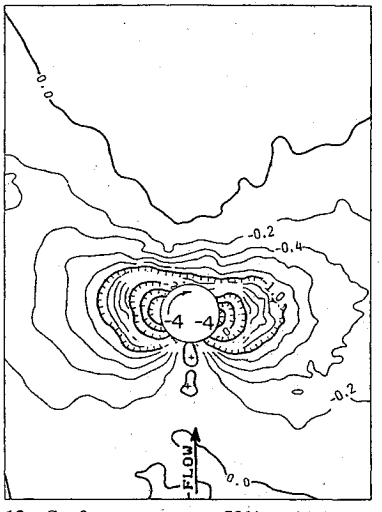

Fig. 13 Surface pressures, 58% swirl jet, $R=8.0$

Naturally, swirl effects are more visible for the 58% swirl case. In Fig. 11, for $R=2.2$ and 58% swirl, it can be seen that the maximum negative pressure at the left rear side is between -8 and -9, whereas the corresponding value for the right side is only between -2 and -3. Increasing the velocity ratio, again, reduced the asymmetry for 58% swirl case (Figs. 12 and 13). However, for this case, the asymmetry induced by swirl is still visible for $R=4$ (Fig. 12).

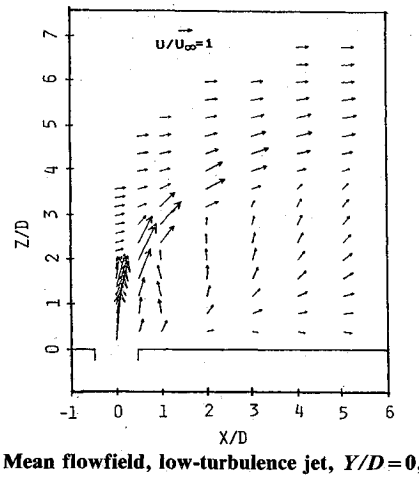

Fig. 14 Mean flowfield, low-turbulence jet, $Y/D=0$, $R=4.0$

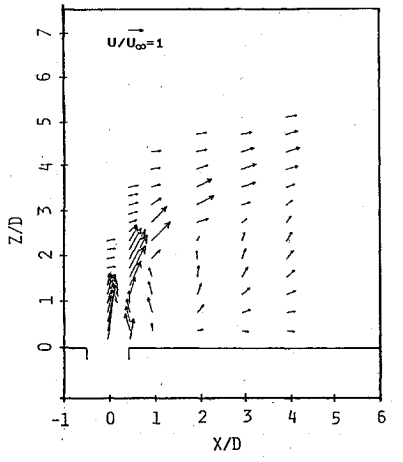

Fig. 15 Mean flowfield, high-turbulence jet, $Y/D=0$, $R=4.0$

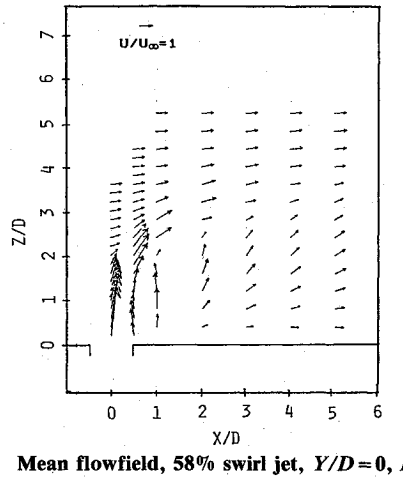

Fig. 16 Mean flowfield, 58% swirl jet, $Y/D=0$, $R=4.0$

In general, swirl has more influence on the area close to the jet exit. It also has more influence for the low-velocity ratios; $R=2.2$ shows the largest swirl effect.

Mean Flowfield Measurements

Mean flowfield results for $R=4$ are presented in Figs. 14–17. The term "penetration height" that will be used here can be defined as the height of the jet center around $X/D=6$ where most of the downstream turning of the jet has occurred. In Figs. 14–16, the results for the jet centerplane ($Y/D=0$) can be seen for the low-turbulence jet, high-turbulence jet, and 58% swirl jet. In Fig. 17, the $X/D=1.026$ cross section is also given for the 58% swirl jet. Data for the 40% swirl jet are available.[7] The penetration height for the low-turbulence jet

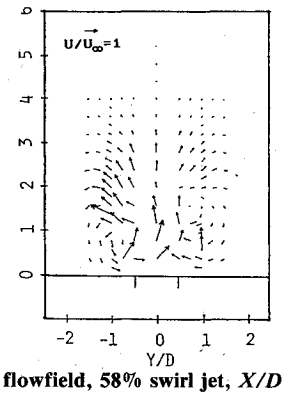

Fig. 17 Mean flowfield, 58% swirl jet, $X/D=1.026$, $R=4.0$

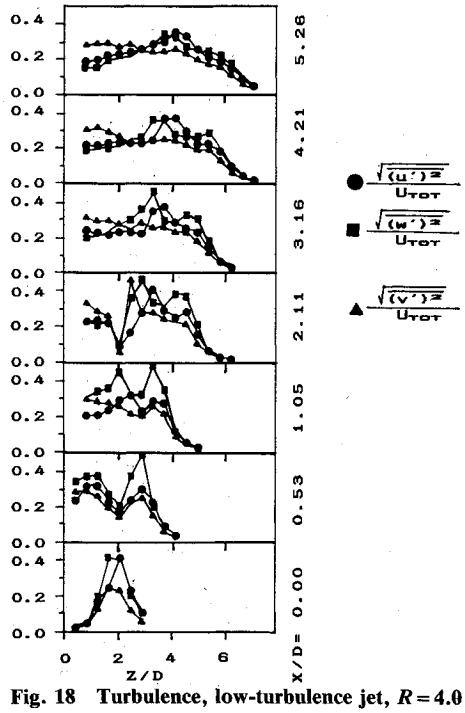

Fig. 18 Turbulence, low-turbulence jet, $R=4.0$

was about $Z/D=5.4$ (Fig. 14), and for the high-turbulence jet about $Z/D=4.9$ (Fig. 15). Comparison of Figs. 14 and 15 shows that the high-turbulence jet entrains more air from the rear.

The penetration height was about $Z/D=5.1$ for 40% swirl and $Z/D=3.6$ for 58% swirl (Fig. 16). The 40% swirl case did not show much difference from the low-turbulence, no-swirl case, but it is clear that the swirl effect is very strong for 58% swirl. For this case, there is more than a 30% reduction in penetration height compared to the low-turbulence, no-swirl case. In Fig. 17 for 58% swirl, the asymmetric vortex formation can be observed. The vortex on the left-hand side of this figure has higher velocities, and its core is closer to the surface. The left-hand side of this figure is the side where swirl velocity and crossflow velocity are in the same direction at the jet exit, and they accelerate each other. The right-hand side of this figure is the side where swirl and crossflow are in opposite directions.

Turbulence Measurements

Turbulence intensities in the X, Y, and Z directions in the plume of the low-exit turbulence jet are presented in Fig. 18 for $R=4$ for the jet centerplane. These results were normalized by the local total mean velocity. Reynolds stress data are also available.[7] This figure can be better understood if it is looked at together with Fig. 14.

For $X/D=0$, locations of $Z/D<0.5$ correspond to the jet core, and turbulence intensities are very low. Locations of

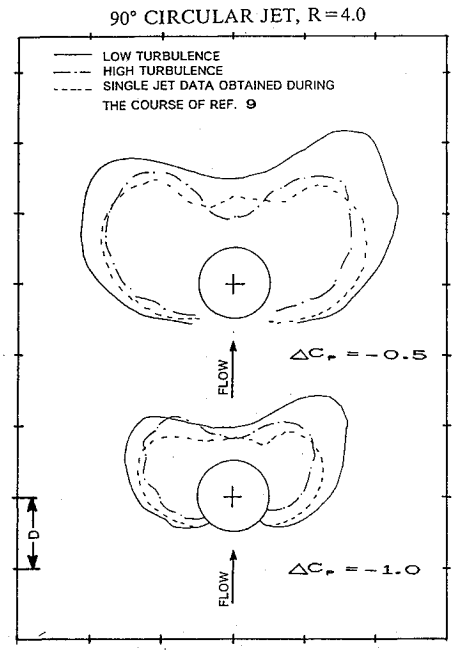

Fig. 19 Surface pressures comparison with Ref. 9, $R=4.0$

Table 2 Comparison of surface pressure, $R=4.0$

Jet type	A_{-1}/A_{exit}	$A_{-0.2}/A_{exit}$
Low turbulence (Fig. 4)	4.31	22.66
High turbulence (Fig. 7)	2.45	13.30
40% swirl (Fig. 9)	3.94	18.72
58% swirl (Fig. 12)	3.94	15.52
90-deg rectangular[11]	1.90	14.33
60-deg rectangular[11]	0.68	10.86

$Z/D>3$ correspond to the freestream, and turbulence intensities are again very low. In $1\leq Z/D\leq 3$ is the region where two flows with 90-deg angle to each other mix, and turbulence intensities above 40% can be observed here. For $X/D=0.53$, $Z/D>4.5$ corresponds to the freestream. $Z/D\cong 3$ is the upper edge of the jet and turbulence intensities are quite large. $Z/D\cong 2$ is more or less the jet core, and turbulence intensities are lower, but it is not such a low-turbulence region as the jet exit. For $Z/D<2$, flow separation, bound vortex formation, and wake effects are important. Going downstream, the turbulence intensities decay, isotropy increases, and the curves get smoother (see $X/D=5.26$ in Fig. 18).

Comparisons

In this section, surface pressure distribution and mean flowfield results of differnt jet types of the present research are compared with each other and other experimental works.

In Table 2, the pressure distribution results of the present work are compared with each other and with the rectangular jet results obtained in a parallel work.[11] These comparisons were made for $R=4$. The rectangular jet of Ref. 11 was aligned streamwise (length-to-width ratio = 4), had low-exit turbulence (= 3%), and was injected at 90 and 60 deg (downward) angles with respect to the model surface. In Table 2, the ratios of the areas covered by the $\Delta C_p=-1$ line and the $\Delta C_p=-0.2$ line to the jet exit area are presented. As can be seen, the negative pressure areas were largest for the low-exit turbulence case. Swirl and especially high-exit turbulence reduced these areas. The rectangular nozzle shape also redued these areas because of less blockage to the crossflow.

In Fig. 19, the low-exit turbulence and high-exit turbulence results of the present work are compared with unpublished single-jet results obtained by Schetz et al. during the course of Ref. 9. The jet of Ref. 9 had a relatively high-exit turbulence level ($\approx$9%) due to a honeycomb flow straightener that was

Table 3 Description of tests for data comparison

Reference	Surface b.l.	Jet exit velocity profile	Jet exit turbulence, %	C_p or ΔC_p	M_{jet}	No. of ports	Port density, near field	Port density, far field
9 (1984)	Turbulent	Uniform nozzle	9	ΔC_p	0.3	—	High	Medium
12 (1965)	Turbulent	Uniform nozzle	—	C_p	0.24	—	—	—
13 (1970)	—	—	—	—	—	—	—	—
14 (1978)	Turbulent	Uniform nozzle	—	ΔC_p	0.4	226	High	Medium
15 (1975)	—	Nozzle	—	ΔC_p	—	—	—	—
Present low turbulence	Turbulent	Uniform nozzle	3	ΔC_p	0.2	>450	High	Medium
Present High turbulence	Turbulent	Uniform nozzle	> 10	ΔC_p	0.1	>450	High	Medium
11 rectangular	Turbulent	Uniform nozzle	3	ΔC_p	0.2	930	Very high	Medium

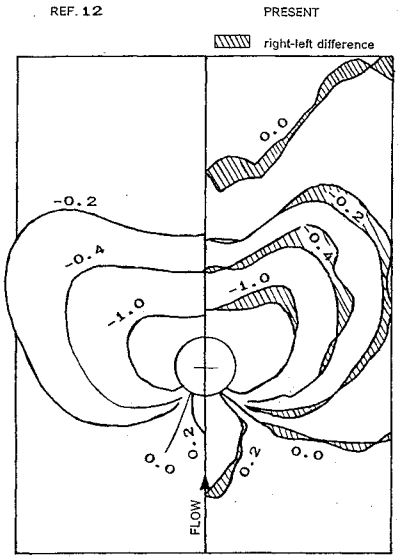

Fig. 20 Surface pressures comparison with Ref. 12, $R=4.0$

uniformly distributed. In this figure, the areas covered by $\Delta C_p=-1$ and $\Delta C_p=-0.5$ lines are compared for $R=4$. Good agreement between the present high-turbulence (>10%) case and the data of Ref. 9 can be observed.

In Fig. 20, the present low-exit turbulence case is compared with the results of Bradbury and Wood[12] for $R=4$, and good agreement can be seen. Comparisons of the present low-turbulence case for $R=4$ can also be made with the results of Mosher,[13] Kuhlman et al,,[14] and Fearn and Weston.[15] In general, agreement was good except for the region behind the jet. For this region, negative pressures of these three earlier works extended to a larger downstream distance around the centerline. In Table 3, some information is given about the works compared.

Comparisons can also be made for jet centerline trajectories for $R=4$. When the present jet types are compared, the low-exit turbulence case showed the highest penetration. The 40% swirl case did not show much difference from this, but the high-turbulence case and, especially, the 58% swirl case, reduced the penetration height considerably. Comparisons of the present low-turbulence case with other experiments[16-19] and prediction[20] were made (see Ref. 7 for figures). Some scatter exists among the experimental data, which could be attributed to the differences in test conditions and complexity of the flowfield. At $X/D=5$, Kamotani and Greber's jet penetrated about 10% higher than the present case.[18] Kamotani and Greber's jet was incompressible, had uniform velocity profile and 0.3% turbulence. The main difference with the present case was the lower turbulence level (0.3% vs 3%), which might explain the higher penetration.

Concluding Remarks

In this work, the effects of high-exit turbulence and swirl on the surface pressure distribution and mean flowfield of a circular jet injected normal to a crossflow have been investigated. In summary, it has been found that high-exit turbulence reduced the size of negative pressure areas on the surface, and it also reduced the jet penetation. Swirl induced asymmetric pressure distributions, particularly for low-velocity ratios ($R=2.2$), high-swirl ratios (58%), and for regions close to the jet exit. Swirl also reduced the penetration height.

Some general comments can be made as a result of the present research:

1) A high-turbulence jet mixes faster, and the potential core region found in a low-turbulence jet does not exist. Blockage effect of a high-turbulence jet will be lesser. These may explain the lower penetration and reduced negative pressure areas.

2) Swirl shortens the length of the potential core, and it may induce turbulence in the jet. The way swirl is introduced into the jet can be considered as important, and it may affect the velocity and turbulence profiles and, thus, the pressure distribution and mean flowfield. For the present research, swirl was introduced by tangential air injection upstream of a contraction that was placed before the jet exit.

3) Swirl induces large asymmetries in the surface pressure distributions. This should not be confused with the slight asymmetry seen for the low-turbulence jet at the lowest velocity ratio ($R=2.2$) (compare Fig. 3 with Figs. 8 and 11). In the latter case, the asymmetry happened probably because of the great sensitivity of the flowfield to small imperfections in the jet exit flow at low-velocity ratios, which might need further investigation.

Acknowledgments

This work was supported by NASA Ames Research Center, Mr. K. Aoyagi, Technical Monitor. The authors would also like to thank Dr. A. K. Jakubowski for his discussions.

References

[1]Abramovich, G. N., *The Theory of Turbulent Jets,* MIT Press, Cambridge, MA, 1960 (English edition).

[2]Lee, C. C., "A Review of Research on the Interaction of a Jet with an External Cross Stream," Brown Engineering Co., Tech. Note R-184, March 1966 (available from DCC as AD 630 294).

[3]Garner, J E., "A Review of Jet Efflux Studies Application to V/STOL Aircraft," U.S. Air Force, Arnold Engineering Develop-

ment Center-TR-67-163, Sept. 1967 (available from DDC as AD 658 432).

[4]Schetz, J. A., *Progress in Astronautics and Aeronautics: Injection and Mixing in Turbulent Flow,* Vol. 68, AIAA, New York, 1980.

[5]Perkins, S. C., Jr., and Mendenhall, M. R., "A Study of Real Jet Effects on the Surface Pressure Distribution Induced by a Jet in a Crossflow," NASA CR-166150 (N81-23029), March 1981.

[6]Crabb, D., Durao, D. F. G., and Whitelaw, J. H., "A Round Jet Normal to a Crossflow," *Journal of Fluids Engineering, Transactions of the ASME,* Vol. 103, March 1981, pp. 142–152.

[7]Kavsaoglu, M. S., "Jets in a Crossflow Including the Effects of Dual Arrangements, Angle, Shape, Swirl and High Turbulence," Ph.D. Dissertation, Virginia Polytechnic Institute and State Univ., Blacksburg, VA, 1987.

[8]Schetz, J.A., Jakubowski, A. K., and Aoyagi, K., "Jet Trajectories and Surface Pressures Induced on a Body of Revolution with Various Dual Jet Configurations," *Journal of Aircraft,* Vol. 20, Nov. 1983, pp. 975–982.

[9]Schetz, J. A., Jakubowski, A. K., and Aoyagi, K., "Surface Pressures Induced on a Flat Plate with In-Line and Side-by-Side Dual Jet Configurations," *Journal of Aircraft*, Vol. 21, July 1984, pp. 484–490.

[10]Moore, C. L. and Schetz, J. A., "Effects of Nonuniform Velocity Profiles on Dual Jets in a Crossflow," AIAA Paper 85-1674, July 1985.

[11]Kavsaoglu, M. S., Schetz, J. A., and Jakubowski, A. K., "Rectangular Jets in a Crossflow," *Journal of Aircraft* (to be published).

[12]Bradbury, L. J. S. and Wood, M. N., "The Static Pressure Distribution around a Circular Jet Exhausting Normally from a Plane Wall into an Airstream," Aeronautical Research Council, CP-822, 1965.

[13]Mosher, D. K., "An Experimental Investigation of a Turbulent Jet in a Cross Flow," Ph.D. Thesis, Georgia Inst. of Technology, Atlanta, GA, Rept. GIT-AER-70-715, (Ph.D. Thesis), Dec. 1970.

[14]Kuhlman, J. M., Ousterhout, D. S., and Warcup, R. W., "Experimental Investigation of Effect of Jet Decay Rate on Jet-Induced Pressures on a Flat Plate," NASA CR-2979, April 1978.

[15]Fearn, R. L. and Weston, R. P, "Induced Pressure Distribution of a Jet in a Crossflow," NASA TN D-7916, June 1975.

[16]Jordinson, R., "Flow in a Jet Directed Normal to the Wind," Aeronautical Research Council, Memorandum 3074, 1956.

[17]Keffer, J. F. and Baines, W. D., "The Round Turbulent Jet in a Cross Wind," *Journal of Fluid Mechanics,* Vol. 15, April 1963, pp. 481–497.

[18]Kamotani, Y. and Greber, I., "Experiments on a Turbulent Jet in Cross-Flow," *AIAA Journal,* Vol. 10, Nov. 1972, pp. 1425–1429.

[19]Chassaing, P., George, J., Claria, A., and Sananes, F., "Physical Characteristics of Subsonic Jets in a Cross-Stream," *Journal of Fluid Mechanics,* Vol. 62, Jan. 1974, pp. 41–64.

[20]Campbell, J. F. and Schetz, J. A., "Flow Properties of Submerged Heated Effluents in a Waterway," *AIAA Journal*, Vol. 11, Feb. 1973, pp. 223–230.

[21]Chien, C. J. and Schetz, J. A., "Numerical Solution of Three-Dimensional Navier-Stokes Equations with Application to Channel Flows and a Buoyant Jet in a Cross-Flow," *Journal of Applied Mechanics,* Vol. 42, Sept. 1975, pp. 575–579.

[22]Oh, T. S. and Schetz, J. A., "Finite-Element Simulation of Jets in a Crossflow with Complex Nozzle Configurations for V/STOL Applications," AIAA Paper 88-3269, July 1988.

[23]Weston, R. P. and Thames, F. C., "Properties of Aspect Ratio 4.0 Rectangular Jets in a Subsonic Crossflow," *Journal of Aircraft,* Vol. 16, Oct. 1979, pp. 701–707.

[24]Jakubowski, A. K., Schetz, J. A., Moore, C. L., and Joag, R., "Effects of Velocity Profile and Inclination on Dual-Jet-Induced Pressures on a Flat Plate in a Crosswind," NASA CR-177361, Oct. 1985.